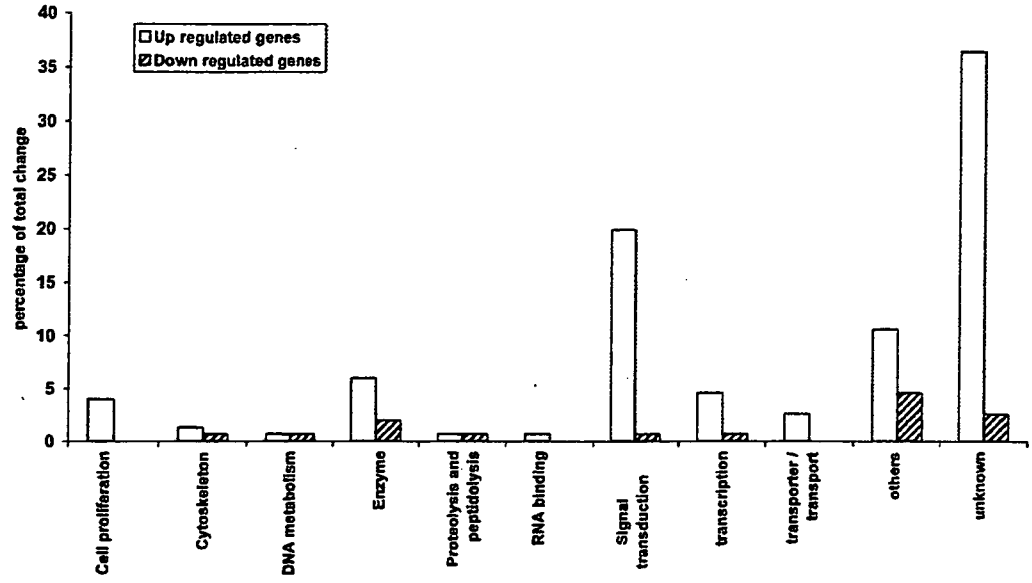

Fig. 2. Effect of BCH on gene expression after 3 h. Expression of many genes altered in T24 cells treated with BCH for 3 h.

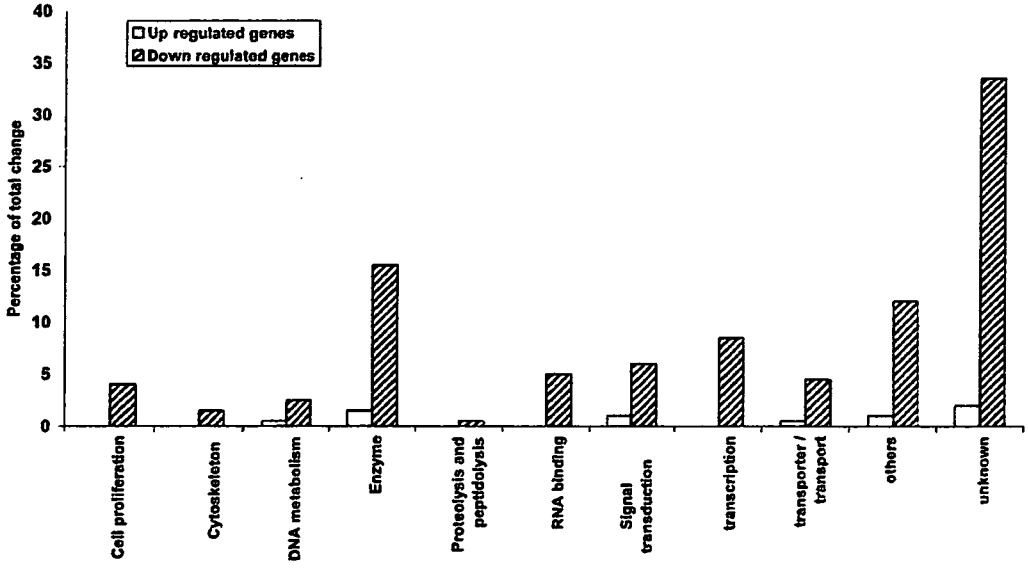

Fig 3. Effect of BCH on gene expression after 12 h. Expression of many genes altered in T24 cells treated with BCH for 12 h.

pendent experiments showed the altered expression of 151 and 200 genes at the mRNA level after 3 and 12 h BCH treatment. Among these genes, 132 and 13 were up-regulated and 19 and 187 were down-regulated by 3 and 12 h BCH treatment respectively. Expression of genes altered as early as 3 and 12 h of BCH treatment and was significantly up-regulated after 3 h and down-regulated after 12 h (Figs. 2 and 3). We found that after 3 h, BCH up-regulated genes that are involved mainly in signal transduction, enzyme reaction, transcription, cell proliferation and transport (Table I). On the other hand after 12 h, BCH down-regulated genes that are related mainly to enzyme reaction, transcription, signal transduction, RNA binding, transport, cell proliferation and DNA metabolism (Table II).

DISCUSSION

For continuous growth and proliferation, rapidly dividing tumor cells require more supply of sugars and amino acids. They are supported by the up regulation of transporters specialized for those nutrients. Transporters for essential amino acids are particularly important since they

Table I. Fold changes of specific genes in T24 cells treated with BCH for 3 h

genes	foldchange	t-test p-value
signal transduction		
Hypothetical protein	3.100	0.156
th79e05.x1 Soares_NhHMPu_S1 Homo sapiens cDNA clone IMAGE:2124896 3', mRNA sequence.	2.871	0.045
Sorting nexin 11	2.691	0.012
GABA(A) receptor-associated protein like 1	2.674	0.083
Down syndrome critical region gene 1	2.666	0.058
Interleukin 8	2.629	0.123
wd41c03.x1 Soares_NFL_T_GBC_S1 Homo sapiens cDNA clone IMAGE:2330692 3' similar to TR:O00538 O00538 F25B3.3 KINASE LIKE PROTEIN. ;, mRNA sequence.	2.596	0.439
Interleukin 8	2.534	0.087
IL2-inducible T-cell kinase	2.526	0.371
Protein kinase C, beta 1	2.427	0.151
Insulin-like growth factor binding protein 3	2.377	0.130
Vav 3 oncogene	2.267	0.053
Fibroblast growth factor 12B	2.237	0.127
CD53 antigen	2.216	0.106
MAD (mothers against decapentaplegic, Drosophila) homolog 7	2.194	0.073
GRO2 oncogene	2.186	0.020
G protein-coupled receptor 27	2.178	0.308
Adhesion glycoprotein	2.173	0.061
qq08e12.x1 Soares_NhHMPu_S1 Homo sapiens cDNA clone IMAGE:1931950 3', mRNA sequence.	2.159	0.027
Epiregulin	2.152	0.021
Gamma-aminobutyric acid (GABA) receptor, rho 2	2.143	0.159
DKFZP564L0862 protein	2.125	0.505
Insulin-like growth factor binding protein 1	2.080	0.216
GTP-binding protein overexpressed in skeletal muscle	2.074	0.056
Syntrophin, gamma 1	2.053	0.388
Adenosine A1 receptor	2.046	0.024
Inhibin, alpha	2.020	0.003
Frizzled (Drosophila) homolog 7	2.008	0.055
601763146F1 NIH_MGC_20 Homo sapiens cDNA clone IMAGE:4026010 5', mRNA sequence.	2.008	0.101
enzyme		
Cytosolic beta-glucosidase	2.668	0.209
UDP glycosyltransferase 1 family, polypeptide A1	2.355	0.014
wg36d09.x1 Soares_NSF_F8_9W_OT_PA_P_S1 Homo sapiens cDNA clone IMAGE:2367185 3', mRNA sequence.	2.287	0.072
Arginase, liver	2.201	0.339
Peptidylprolyl isomerase A (cyclophilin A)	2.166	0.423
ov13a06.x1 NCI_CGAP_Kid3 Homo sapiens cDNA clone IMAGE:1637170 3' similar to WP:R07B7.5 CE06267 ;, mRNA sequence.	2.116	0.270
cytochrome P450IIE1; Human cytochrome P450IIE1 (ethanol-inducible) gene, complete cds.	2.075	0.279
Keratin, hair, basic, 6 (monilethrix)	2.072	0.043
Protein kinase, Y-linked	2.028	0.430
transcription		
Homeo box A6	2.294	0.062
yf31g02.s1 Soares fetal liver spleen 1NFLS Homo sapiens cDNA clone IMAGE:128498 3', mRNA sequence.	2.024	0.259
Runt-related transcription factor 2	2.009	0.048

Table I. Continued

genes	foldchange	t-test p-value
transcription		
Cardiac-specific homeo box	2.095	0.170
wa17f11.x1 NCI_CGAP_Kid11 Homo sapiens cDNA clone IMAGE:2298381 3' similar to TR:Q15886 Q15886 X-LINKED NUCLEAR PROTEIN ;, mRNA sequence.	2.435	0.276
Cofactor required for Sp1 transcriptional activation, subunit 3 (130kD)	2.376	0.132
Wolf-Hirschhorn syndrome candidate 1-like 1	2.047	0.013
cell proliferation		
Tumor necrosis factor receptor superfamily, member 9	2.651	0.084
Interleukin 1, beta	2.233	0.001
Interleukin 1, alpha	2.150	0.019
Interleukin 12A (natural killer cell stimulatory factor 1, cytotoxic lymphocyte maturation factor 1, p35)	2.124	0.162
Epidermal growth factor receptor (avian erythroblastic leukemia viral (v-erb-b) oncogene homolog)	2.093	0.066
nad20g10.x1 NCI_CGAP_Lu24 Homo sapiens cDNA clone IMAGE:3366330 3', mRNA sequence.	2.031	0.087
transport		
Solute carrier family 4, sodium bicarbonate cotransporter-like, member 10	3.528	0.166
UI-H-BW0-ajo-f-12-0-UI.s1 NCI_CGAP_Sub6 Homo sapiens cDNA clone IMAGE:2732686 3', mRNA sequence.	2.468	0.423
Solute carrier family 35 (UDP-N-acetylglucosamine (UDP-GlcNAc) transporter), member 3	2.110	0.152
Solute carrier family 21 (organic anion transporter), member 3	2.031	0.030

Table II. Fold changes of specific genes in T24 cells treated with BCH for 12 h

gene	foldchange	t-test p-value
enzyme		
GDP-mannose pyrophosphorylase B	0.306	0.078
AU121975 MAMMA1 Homo sapiens cDNA clone MAMMA1001393 5', mRNA sequence.	0.319	0.235
Polymerase (DNA directed), mu	0.334	0.159
Adenylate kinase 2	0.353	0.015
F-box only protein 9	0.362	0.057
Stearoyl-CoA desaturase (delta-9-desaturase)	0.362	0.046
N-myristoyltransferase 1	0.370	0.095
Protein phosphatase 2 (formerly 2A), regulatory subunit B" (PR 72), alpha isoform and (PR 130), beta isoform	0.383	0.078
Homo sapiens Scd mRNA for stearoyl-CoA desaturase, complete cds.	0.384	0.009
qd05f07.x1 Soares_placenta_8to9weeks_2NbHP8to9W Homo sapiens cDNA clone IMAGE:1722853 3' similar to SW:ER19_HUMAN P53602 DIPHOSPHOMEVALONATE DECARBOXYLASE ;contains MER22.b1 MSR1 repetitive element ;, mRNA sequence.	0.404	0.013
602022620F1 NCI_CGAP_Brn67 Homo sapiens cDNA clone IMAGE:4158005 5', mRNA sequence.	0.406	0.020
N-acetylglucosaminidase, alpha- (Sanfilippo disease IIIB)	0.407	0.279
3-hydroxybutyrate dehydrogenase (heart, mitochondrial)	0.409	0.238
Creatine kinase, mitochondrial 2 (sarcomeric)	0.440	0.135
Phosphodiesterase 4D, cAMP-specific (dunce (Drosophila)-homolog phosphodiesterase E3)	0.441	0.020
qi08f09.x1 Soares_NhHMPu_S1 Homo sapiens cDNA clone IMAGE:1855913 3', mRNA sequence.	0.454	0.071
AL525798 LTI_NFL003_NBC3 Homo sapiens cDNA clone CS0DC013YB08 5 prime, mRNA sequence.	0.454	0.020
KIAA0015 gene product	0.455	0.043
Glutaryl-Coenzyme A dehydrogenase	0.467	0.082
Polynucleotide kinase 3'-phosphatase	0.470	0.079
Enolase 2, (gamma, neuronal)	0.471	0.008
xn86c10.x1 Soares_NFL_T_GBC_S1 Homo sapiens cDNA clone IMAGE:2701362 3' similar to TR:Q99766 Q99766 HYPOTHETICAL 15.7 KD PROTEIN. ; mRNA sequence.	0.481	0.112

Table II. Continued

gene	foldchange	t-test p-value
enzyme		
Serine hydroxymethyltransferase 1 (soluble)	0.483	0.092
Crystallin, zeta (quinone reductase)-like 1	0.486	0.042
xd94e03.x1 Soares_NFL_T_GBC_S1 Homo sapiens cDNA clone IMAGE:2605276 3' similar to WP:Y116A8C.27 CE23335 ;, mRNA sequence.	0.488	0.213
Aminoacylase 1	0.488	0.016
H.sapiens pseudogene for mitochondrial ATP synthase c subunit (P2 form).	0.491	0.088
zi27a06.s1 Soares_fetal_liver_spleen_1NFLS_S1 Homo sapiens cDNA clone IMAGE:431986 3', mRNA sequence.	0.491	0.061
Fatty-acid-Coenzyme A ligase, long-chain 3	0.492	0.069
Triosephosphate isomerase 1	0.494	0.322
Tumor necrosis factor receptor superfamily, member 6b, decoy	0.495	0.000
transcription		
Paired box gene 3 (Waardenburg syndrome 1)	0.342	0.260
Paired box gene 8	0.423	0.218
AU118165 HEMBA1 Homo sapiens cDNA clone HEMBA1003008 5', mRNA sequence.	0.466	0.057
Core promoter element binding protein	0.447	0.016
Death effector domain-containing	0.484	0.028
Trinucleotide repeat containing 11 (THR-associated protein, 230 kDa subunit)	0.498	0.002
NS1-binding protein	0.335	0.018
Hypothetical protein	0.484	0.031
602437464F1 NIH_MGC_46 Homo sapiens cDNA clone IMAGE:4555622 5', mRNA sequence.	0.486	0.027
601872674F1 NIH_MGC_54 Homo sapiens cDNA clone IMAGE:4096483 5', mRNA sequence.	0.432	0.002
Cofactor required for Sp1 transcriptional activation, subunit 9 (33kD)	0.472	0.157
Zinc finger protein 254	0.489	0.374
Ring finger protein 1	0.404	0.154
Nuclear respiratory factor 1	0.376	0.111
HSPC028 protein	0.486	0.009
KIAA0664 protein	0.496	0.031
signal transduction		
Regulator of G-protein signalling 4	0.109	0.029
Integrin, alpha 9	0.164	0.015
CAMP responsive element modulator	0.255	0.158
Endothelin receptor type B	0.302	0.011
AL514445 LTI_NFL006_PL2 Homo sapiens cDNA clone CL0BB010ZF08 3 prime, mRNA sequence.	0.322	0.008
Ankyrin 1, erythrocytic	0.340	0.094
wu94e06.x1 NCI_CGAP_Kid3 Homo sapiens cDNA clone IMAGE:2527714 3' similar to gb:U07358 MIXED LINEAGE KINASE 2 (HUMAN);, mRNA sequence.	0.342	0.098
ADP-ribosylation factor related protein 1	0.345	0.030
Melanoma cell adhesion molecule	0.351	0.053
7o43e03.x1 NCI_CGAP_Kid11 Homo sapiens cDNA clone IMAGE:3577036 3', mRNA sequence.	0.431	0.095
LIM domain only 7	0.439	0.045
Enigma (LIM domain protein)	0.492	0.036
RNA binding		
qb33c06.x1 Soares_pregnant_uterus_NbHPU Homo sapiens cDNA clone IMAGE:1698058 3', mRNA sequence.	0.215	0.055
RNA binding motif protein 12	0.386	0.007

Table II. Continued

gene	foldchange	t-test p-value
RNA binding		
Polyadenylate binding protein-interacting protein 1	0.411	0.029
Splicing factor, arginine/serine-rich 6	0.419	0.003
AU146237 HEMBA1 Homo sapiens cDNA clone HEMBA1007233 3', mRNA sequence.	0.422	0.013
Polyadenylate binding protein-interacting protein 1	0.458	0.058
Splicing factor, arginine/serine-rich 7 (35kD)	0.472	0.060
DEAD-box protein abstrakt	0.493	0.035
Mitochondrial ribosomal protein L12	0.495	0.138
Heterogeneous nuclear ribonucleoprotein D-like	0.497	0.025
transport		
wc46f12.x1 NCI_CGAP_Pr28 Homo sapiens cDNA clone IMAGE:2321711 3' similar to TR:O14564 O14564 HYPOTHETICAL 67.1 KD PROTEIN. ;, mRNA sequence.	0.338	0.072
Uncoupling protein 2 (mitochondrial, proton carrier)	0.385	0.020
Adaptor-related protein complex 3, sigma 2 subunit	0.278	0.110
Solute carrier family 4, anion exchanger, member 2 (erythrocyte membrane protein band 3-like 1)	0.408	0.134
Hypothetical protein FLJ14038	0.469	0.002
Solute carrier family 4, sodium bicarbonate cotransporter-like, member 10	0.395	0.124
N amino acid transporter 3	0.451	0.072
Solute carrier family 25 (mitochondrial carrier; oxoglutarate carrier), member 11	0.467	0.017
Solute carrier family 19 (folate transporter), member 1	0.490	0.068
cell proliferation		
Deoxyhypusine synthase	0.175	0.026
Deoxyhypusine synthase	0.372	0.039
ba69f11.x1 NIH_MGC_20 Homo sapiens cDNA clone IMAGE:2905677 3' similar to SW:CL6_RAT Q08755 INSULIN-INDUCED GROWTH RESPONSE PROTEIN CL-6 ;, mRNA sequence.	0.437	0.008
Cyclin H	0.455	0.043
Bridging integrator 1	0.487	0.071
V-Ki-ras2 Kirsten rat sarcoma 2 viral oncogene homolog	0.489	0.171
Deoxyhypusine synthase	0.494	0.031
U69567 Soares infant brain 1NIB Homo sapiens cDNA clone c-2mell, mRNA sequence.	0.499	0.072
DNA metabolism		
BRCA1-interacting protein 1; BRCA1-associated C-terminal helicase 1	0.410	0.028
Uracil-DNA glycosylase	0.434	0.102
Nth (E.coli endonuclease III)-like 1	0.443	0.017
DNA (cytosine-5-)-methyltransferase 2	0.469	0.209
602504673F1 NIH_MGC_77 Homo sapiens cDNA clone IMAGE:4617907 5', mRNA sequence.	0.470	0.200

are indispensable for protein synthesis (Christensen, 1990; McGivan and Pastor-Anglada, 1994). Among the amino acid transport systems described, system L is a major rout for providing cells with large neutral amino acids including branched or aromatic amino acids (Cornford *et al.*, 1992; Gomes and Soares-da-Silva, 1999). LAT1 is a system L amino acid transporter which transports a lot of essential amino acids. It is proposed to be at least one of the amino acids transporters essential for tumor cell growth (Yanagida *et al.*, 2001). High level of expression of LAT1 in tumor cells was indicated in tumor masses of various tissue origins as well as various tumor cell lines to support the high protein synthesis for cell growth and cell activation (Kanai *et al.*, 1998; Sang *et al.*, 1995; Wolf *et al.*, 1996). Since LAT1 is an amino acid transporter essential for tumor cell growth, one can expect that inhibition of LAT1 function may be a rational to anti-cancer therapy to suppress tumor growth (Kim *et al.*, 2004). BCH

is an amino acid-related compound which has been used as a selective inhibitor of system L (Christensen, 1990; Christensen *et al.*, 1969). Our previous studies have shown that BCH exert inhibitory effects on T24 cells through inhibition of LAT1 (Kim *et al.*, 2002). We confirmed this for T24 cells by showing that BCH in logarithmic phase of cell growth curve inhibits cell proliferation (Fig. 1).

Determining of gene expression profiles of T24 bladder carcinoma cells after BCH treatment is important for designing new anticancer drugs. It is possible to analyze the expression profiles of a large number of genes simultaneously using microarray. In this study, we utilized the high throughput gene chip, which contains 39,000 known genes, to determine the alternation of gene expression profiles of T24 bladder carcinoma cells exposed to BCH. Our results from cDNA microarray provided a complex cellular and molecular response to BCH treatment that likely to be mediated by a variety of regulatory pathways. We found that the molecular response to BCH in T24 bladder carcinoma cells involved inhibition or induction of genes that are related to biochemical, biological and regulatory processes in the cells. These genes have specific functions in cell proliferation, DNA metabolism, enzyme reaction, RNA binding, signal transduction, transcription, and transport. General tendency was up-regulation of these genes at 3 h and down-regulation at 12 h after BCH treatment (Fig. 2 and 3). These results suggest that inhibition of LAT1 by BCH may modulate the expression of first-response genes at an earlier stage (3 h), and in turn, alter the expression of intracellular second messenger molecules, resulting in cell adaptation for survival. At later stage (12 h), cellular response to BCH may involve modulation of gene expression for cell growth inhibition. For example up regulation of genes that are involved in cell proliferation at 3 h provide cellular pathways for survival and adaptation whereas down regulation of this group of genes at 12 h inhibit cell growth. Expression of interleukin 1 that stimulates proliferation (Beales, 2002; Kaden *et al.*, 2003; Olman *et al.*, 2002), significantly increased after 3 h and expression of deoxyhypusine synthase that causes growth in mammalian cells (Chen *et al.*, 1996; Park *et al.*, 1994; Shi *et al.*, 1996) decreased after 12 h, suggesting that BCH may inhibit cell growth through regulation of the expression of these important genes related to cell proliferation.

In signal transduction group, up regulation of Sorting nexin 11, GRO2 oncogene, Epiregulin, Adenosine A1 receptor, Inhibin alpha and down regulation of KIAA1075 protein were observed at 3 h whereas down regulation of Regulator of G-protein signalling 4, Integrin alpha 9, Endothelin receptor type B, ADP-ribosylation factor related protein 1, LIM domain only 7, Enigma (LIM domain protein) and up regulation of Hypothetical protein and Opsin 3 (encephalopsin, panopsin) were observed at 12 h, suggesting that cell signal transduction pathways is important for cell growth inhibition *via* LAT1 inhibitor.

In summary, we have analyzed the gene expression profiles of T24 bladder carcinoma cells exposed to BCH. BCH altered the expressions of many genes that are related to the control of cell proliferation, DNA metabolism, enzyme reaction, RNA binding, signal transduction, transcription, and transport. The gene expression profiles revealed novel molecular mechanisms by which BCH exerts its inhibitory effects on bladder carcinoma. BCH-induced regulation of these genes may be exploited for mechanism-based therapeutic strategies and new drugs development for bladder carcinoma. However, further in-depth studies are required to investigate the effects of BCH on the regulation of important cellular molecules at the protein levels to examine the effects of BCH on cellular pathways.

REFERENCES

Beales, I. L., Effect of Interlukin-1â on proliferation of gastric epithelial cells in culture. *BMC Gastroenterol.*, 2, 7 (2002).

Chen, Z. P., Yan, Y. P., Ding, Q. J., Knapp, S., Potenza, J. A., Schugar, H. J., and Chen, K. Y., Effects of inhibitors of deoxyhypusine synthase on the differentiation of mouse neuroblastoma and erythroleukemia cells. *Cancer lett.*, 105, 233-239 (1996).

Christensen, H. N., Role of amino acid transport and countertransport in nutrition and metabolism. *Physiol. Rev.*, 70, 43-77 (1990).

Christensen, H. N., Handlogten, M. E., Lam, I., Tager, H. S., and Zand, R., A bicyclic amino acid to improve discriminations among transport systems. *J. Biol. Chem.*, 244, 1510–1520 (1969).

Cornford, E. M., Young, D., Paxton, J. W., Finlay, G. J., Wilson, W. R., and Pardridge, W. M., Melphalan penetration of the blood-brain barrier via the neutral amino acid transporter in tumor-bearing brain. *Cancer Res.*, 52, 138-143 (1992).

Gomes, P. and Soares-da-Silva, P., L-DOPA transport properties in an immortalised cell line of rat capillary cerebral endothelial cells, RBE 4. *Brain Res.*, 829, 143-150 (1999).

Kaden, J. J., Dempfle, C. E., Grobholz, R., Tran, H. T., Kilic, R., Sarikoc, A., Brueckmann, M., Vahl, C., Hagl, S., Haase, K. K., and Borggrefe, M., Interleukin-1 beta promotes matrix metalloproteinase expression and cell proliferation in calcific aortic valve stenosis. *Atherosclerosis*, 170, 205-211 (2003).

Kanai, Y. and Endou, H., Heterodimeric amino acid transporters: molecular biology and pathological and pharmacological relevance. *Curr. Drug Metab.*, 2, 339-354 (2001).

Kanai, Y., Segawa, H., Miyamoto, K., Uchino, H., Takeda, E., and Endou, H., Expression cloning and characterization of a transporter for large neutral amino acids activated by the

heavy chain of 4F2 antigen (CD98). *J. Biol. Chem.*, 273, 23629–23632 (1998).

Kanno, J., Aisaki, K. I., Igarashi, K., Nakatsu, N., Ono, A., Kodama, Y., and Nagao, T., "Per cell" normalization method for mRNA measurement by quantitative PCR and microarrays. *BMC Genomics*, 7, 64 (2006).

Kim, D. K., Kanai, Y., Choi, H. W., Tangtrongsup, S., Chairoungdua, A., Babu, E., Tachampa, K., Anzai, N., Iribe, Y., and Endou, H., Characterization of the system L amino acid transporter in T24 human bladder carcinoma cells. *Biochim. Biophys. Acta*, 1565, 112-121 (2002).

Kim, D. K., Kim, I. J., Hwang, S., Kook, J. H., Lee, M. C., Shin, B. A., Bae, C. S., Yoon, J. H., Ahn, S. G., Kim, S. A., Kanai, Y., Endou, H., and Kim, J. K., System L-amino acid transporters are differently expressed in rat astrocyte and C6 glioma cells. *Neurosci. Res.*, 50, 437-446 (2004).

Li, Y. and Sarkar, F. H., Gene expression profiles of genistein-treated PC3 prostate cancer cells. *J. Nutr.*, 132, 3623-3631 (2002).

Macgregor, P. F. and Squire, J. A., Application of microarrays to the analysis of gene expression in cancer. *Clin. Chem.*, 48, 1170-1177 (2002).

McGivan, J. D. and Pastor-Anglada, M., Regulatory and molecular aspects of mammalian amino acid transport. *Biochem. J.*, 299, 321-334 (1994).

Olman, M. A., White, K. E., Ware, L. B., Cross, M. T., Zhu, S., and Matthay, M. A., Microarray analysis indicates that pulmonary edema fluid from patients with acute lung injury mediates inflammation, mitogen gene expression, and fibroblast proliferation through bioactive interleukin-1. *Chest*, 121 Suppl 3, 69-70 (2002).

Oxender, D. L. and Christensen, H. N., Evidence for two types of mediation of neutral amino acid transport in Ehrlich cells. *Nature*, 197, 765-767 (1963).

Park, M. H., Wolff, E. C., Lee, Y. B., and Folk, J. E., Antiproliferative effects of inhibitors of deoxyhypusine synthase. Inhibition of growth of Chinese hamster ovary cells by guanyl diamines. *J. Biol. Chem.*, 269, 27827-27832 (1994).

Sang, J., Lim, Y. P., Panzia, M., Finch, P., and Thompson, N. L., TA1, a highly conserved oncofetal complementary DNA from rat hepatoma, encodes an integral membrane protein associated with liver development, carcinogenesis, and cell activation. *Cancer Res.*, 55, 1152-1159 (1995).

Shi, X. P., Yin, K. C., Ahern, J., Davis, L. J., Stern, A. M., and Waxman, L., Effects of N1-guanyl-1, 7-diaminoheptane, an inhibitor of deoxyhypusine synthase, on the growth of tumorigenic cell lines in culture. *Biochim. Biophys. Acta*, 1310, 119-126 (1996).

Wolf, D. A., Wang, S., Panzia, M. A., Bassily, N. H., and Thompson, N. L., Expression of a highly conserved oncofetal gene, TA1/E16, in human colon carcinoma and other primary cancers: homology to Schistosoma mansoni amino acid permease and Caenorhabditis elegans gene products. *Cancer Res.*, 56, 5012-5022 (1996).

Yanagida, O., Kanai, Y., Chairoungdua, A., Kim, D. K., Segawa, H., Nii, T., Cha, S. H., Matsuo, H., Fukushima, J., Fukasawa, Y., Tani, Y., Taketani, Y., Uchino, H., Kim, J. Y., Inatomi, J., Okayasu, I., Miyamoto, K., Takeda, E., Goya, T., and Endou, H., Human L-type amino acid transporter 1 (LAT1): characterization of function and expression in tumor cell lines. *Biochim. Biophys. Acta*, 1514, 291-302 (2001).

ELSEVIER

Experimental Hematology

Experimental Hematology 35 (2007) 1190–1200

Glycolytic inhibition by mutation of pyruvate kinase gene increases oxidative stress and causes apoptosis of a pyruvate kinase deficient cell line

Ken-ichi Aisaki[a], Shin Aizawa[b], Hisaichi Fujii[c], Jun Kanno[a], and Hitoshi Kanno[c,d,e]

[a]*Cellular and Molecular Toxicology Division, National Institute of Health and Sciences, Tokyo, Japan;* [b]*Department of Anatomy, Nihon University School of Medicine, Tokyo, Japan;* [c]*Department of Transfusion Medicine and Cell Processing;* [d]*Institute of Medical Genetics; and* [e]*Division of Genomic Medicine, Department of Advanced Biomedical Engineering and Science, Graduate School of Medicine, Tokyo Women's Medical University, Tokyo, Japan*

(Received 13 November 2006; revised 8 May 2007; accepted 9 May 2007)

Objective. **SLC3 is a Friend erythroleukemic cell line established from the *Pk-1*^{slc} mouse, a mouse model of red blood cell type-pyruvate kinase (R-PK) deficiency. This study was aimed to elucidate the mechanisms attributing to apoptosis induced by R-PK deficiency.**

Materials and Methods. **SLC3 and a control Friend cell line, CBA2, were cultured in a condition of glucose deprivation or supplementation with 2-deoxyglucose, and apoptosis was detected by annexin V. We established two stable transfectants of SLC3 cells with human R-PK cDNA, and examined the effect of R-PK on an apoptotic feature by cell cycle analysis. Intracellular oxidation was measured with 2′,7′-dichlorofluorescin diacetate. DNA microarray analysis was performed to examine gene-expression profiles between the two transfectants and parental SLC3.**

Results. **SLC3 was more susceptible than CBA2 to apoptosis induced by glycolytic inhibition. The forced expression of R-PK significantly decreased cells at the sub G_0/G_1 stage in an expression-level dependent manner. Microarray analysis showed that proapoptotic genes, such as *Bad*, *Bnip3*, and *Bnip3l*, were downregulated in the transfectants. In addition, peroxiredoxin 1 (*Prdx1*) and other antioxidant genes, such as *Cat*, *Txnrd1*, and *Glrx1* were also downregulated. A significant decrease of dichlorofluorescein fluorescence was observed by R-PK expression. Preincubation with a glutathione precursor showed a significant decrease of apoptosis.**

Conclusion. **These results indicated that glycolytic inhibition by R-PK gene mutation augmented oxidative stress in the Friend erythroleukemia cell, leading to activation of hypoxia-inducible factor-1 as well as downstream proapoptotic gene expression. Thus, R-PK plays an important role as an antioxidant during erythroid differentiation.** © **2007 ISEH - Society for Hematology and Stem Cells. Published by Elsevier Inc.**

Glycolysis is an essential metabolic pathway in all organisms. Pyruvate kinase (PK) is a key glycolytic enzyme, and has four isoenzymes in mammals, designated M_1, M_2, L (liver), and R (red blood cell). In humans, these isozymes are encoded by two structural genes, *PKM* and *PKLR*, respectively [1]. M_2-PK is the only isozyme that is active in early fetal tissues and also almost ubiquitously expressed in adult tissues, including hematopoietic stem cells, progenitors, leukocytes, and platelets. Red blood cell type-pyruvate kinase (R-PK) becomes a major isozyme during erythroid differentiation/maturation [2,3], and in mature red blood cells (RBCs), R-PK is the only detectable PK isozyme. Deficiency of R-PK causes shortened RBC survival, resulting in hemolytic anemia. In humans, PK deficiency is the most prevalent glycolytic enzyme defect, which is responsible for hereditary hemolytic anemia [4,5].

We have previously established SLC3 [6], a line of Friend erythroleukemic cells from the *Pk-1*^{slc} mouse [7], which has chronic hemolytic anemia with marked splenomegaly due to a missense mutation of the murine *Pklr* gene [8]. SLC3 showed spontaneous apoptosis during routine passage and in vitro erythroid differentiation by butyrate exacerbated apoptosis of SLC3 [6]. Recently, we examined the spleen of a subject with severe PK deficiency [9], and discovered enhanced extramedullary hematopoiesis as well as apoptotic erythroid cells. Enhanced apoptosis

Offprint requests to: Hitoshi Kanno, M.D. Ph.D., Department of Transfusion Medicine and Cell Processing, Tokyo Women's Medical University, Tokyo 162-8666, Japan.

0301-472X/07 $–see front matter.
doi: 10.1016/j.exphem.2007.05.005

was also identified in TER119-positive erythroid cells isolated from *Pk-1*^{slc} mice [10]. These results provide evidence that the metabolic disturbances in PK deficiency affect not only the survival of RBCs but also the maturation of erythroid progenitors, which results in apoptosis.

In this study, we examined whether Friend erythroleukemic cell lines showed apoptosis when glycolysis was inhibited. To evaluate whether overexpression of the normal R-PK gene ameliorated apoptosis, we established stable transfectants of SLC3 and compared their apoptotic characteristics and transcriptional profiles with parental SLC3. We present here several pieces of evidence, revealing the biological significance of R-PK to suppress oxidative stress during erythroid differentiation.

Materials and methods

Cell culture and flow cytometric analysis

Friend erythroleukemic cell lines SLC3 and CBA2 have been described previously [6]. Both cell lines are maintained in Iscove's modified Dulbecco's medium (Invitrogen, Carlsbad, CA, USA) supplemented with 10% heat-inactivated fetal calf serum, 20 μM 2-mercaptoethanol, and a mixture of penicillin-streptomycin (Sigma-Aldrich, St Louis, MO, USA).

To evaluate the adverse effects of glycolytic inhibition, cells were cultured in either glucose-free RPMI-1640 (Invitrogen) or RPMI-1640 with 2-deoxyglucose (2-DG) at final concentrations of 0.1, 1, and 10 mM. Iscove's modified Dulbecco's medium containing 110 mg/L sodium pyruvate, and RPMI-1640 containing no pyruvate.

Flow cytometric analysis was performed by EPICS XL and analyzed with software, EXPO32 ADC (Beckman-Coulter, Fullerton, CA, USA). Annexin V-Alexa568 and rhodamine 123 were obtained from Roche Diagnostics (Basel, Switzerland) and Sigma, respectively. To examine the effect of N-acetyl-L-cysteine upon apoptosis, we preincubated cells in RPMI-1640 supplemented with 10 mM N-acetyl-L-cysteine for 12 hours, followed by 12- to 24-hour incubation with RPMI-1640.

Establishment of stable transfectants expressing normal R-PK in SLC3 cells

We constructed a human R-PK cDNA expression plasmid vector in erythroid cells. A 1.7-kb fragment covering the entire coding region of human R-PK cDNA [11] was introduced into *KpnI-EcoRV* sites of pcDNA3.1 (Invitrogen). Plasmid DNA was purified with an EndoFree Maxi DNA purification kit (Qiagen, Hilden, Germany). Transfection was done with Effectene Transfection Reagent (Qiagen) as indicated by the manufacturer. Transfected cells were selected using G418 (400 μg/mL).

RT-PCR, Western blotting, and enzyme assay

Total cellular RNA was extracted with an RNeasy purification kit (Qiagen), and 2 μg RNA was reverse-transcribed (RT) at 42°C for 90 minutes with 50 pmole oligo (dT)17 primer, 0.5 U/μL cloned RNase inhibitor (Takara Bio, Shiga, Japan), 10 mM dithiothreitol, 1 mM deoxyribonucleoside triphosphate, and 50 U Expand Reverse Transcriptase (Roche Diagnostics). Aliquots (1/10) were subjected to PCR using primer pairs specifically amplified with human and murine R-PK cDNA, hRPK-F (5′-TGGCCCAGC CTACCCTTGTA-3′)/hRPK-R (5′-CTTAAAGGTGGGGCTTTG GA-3′) and mRPK-F (5′-GCAGATGATGTGGACCGAAG-3′)/ mRPK-R (5′-CTAGATGGCAGATGTGGGACTA-3′), respectively. The reaction mixtures were subjected to 40 cycles of amplification consisting of 94°C for 20 seconds, 60°C for 10 seconds, and 72°C for 10 seconds for hRPK and 94°C for 20 seconds, 60°C for 20 seconds, and 72°C for 20 seconds for mRPK in a GeneAmp PCR system 2400 (Roche Diagnostics, Switzerland), and separated using 2% agarose gel electrophoresis.

For Western blot analysis, cells were harvested, followed by washing with phosphate-buffered saline twice. Following three-times freezing and thawing in extraction buffer (10 mM Tris/ HCl, pH 8.0, 10 mM $MgCl_2$, 0.003% 2-mercaptoethanol, 0.02 mM ethylenediamine tetraacetic acid), cell extracts were obtained for Western blot analysis. Protein assays were performed by the method of Bradford using a commercial kit (Bio-Rad Laboratories, Hercules, CA, USA).Western blot analysis was conducted using anti-rat L-PK (kindly provided Tamio Noguchi, Nagoya University) and ECL advance Western Blotting Detection Kit (Amersham Biosciences, Buckinghamshire, UK).

PK and lactate dehydrogenase (LDH) activity was measured, as described [12].

Microarray analysis

To prepare high-quality total cellular RNA for the GeneChip assay, RNA was extracted with modified protocols using the TRIzol LS (Invitrogen) and RNeasy purification kit (Qiagen). Briefly, cells were harvested with no washing step, and immediately homogenized with the RLT buffer. The lysate was then mixed with 3 volumes of the TRIzol LS. After a 10-minute incubation at room temperature, the sample solution was mixed with an equal volume of chloroform. The sample was centrifuged at 10,000*g* for 15 minutes at 4°C, and then the upper aqueous phase was transferred to a fresh tube. After mixing with an equal volume of 70% ethanol, the sample was incubated for 10 minutes at room temperature. Without any flash step, the sample solution was transferred to the RNeasy column, and then processed by the manufacturer recommended protocol.

To normalize the variation in data based on the cell count, we used *Bacillus subtilis* RNA for an external standard signal, which was added to the cell lysate in proportion to the sample's DNA contents [13]. Ten microliters of cell lysate was provided for DNA quantification using Picogreen (Invitrogen). GeneChip (Affymetrix, Santa Clara, CA, USA) analysis was carried out according to the Affymetrix-recommended protocols. Processed RNA was hybridized to the Affymetrix Murine Genome 430A arrays (22960 probe sets). Signal values were calculated from scanned images by the Affymetrix Microarray Operation System (GCOS). The cell sample was pooled from six culture dishes at each condition and one GeneChip was used per one pooled sample.

Data analysis

Data were normalized by an original program (SCal), which processes data in proportional conversion based on the DNA content of each biosample [13]. This DNA content-based normalization method improves the measurement accuracy of GeneChip. For example, a series of samples was measured by quantitative PCR and Affymetrix GeneChip microarrays using this method, and the results showed up to 90% concordance [13].

To identify differentially expressed genes, we used an empirical threshold calculated by an original algorithm (Fx). The Fx threshold is based on the signal intensity level and is calculated as follows: $Y = X \cdot (1 + RC^{(w\text{-}\log X)})$ and $Y = X \cdot (1 + C^{(w\text{-}\log X)})^{-1}$ (Fx1 and Fx2 respectively; C and w are constant parameters reflecting actual measurement data by GeneChip hybridized with the standard sample). C and w were set to 3.0 and 2.5, respectively, which was equivalent to $p < 0.02$. In the scatter plot, the spots above the Fx1 line were evaluated as upregulated, and the spots below the Fx2 line were evaluated as downregulated.

Results

SLC3 is more susceptible than the control to apoptosis due to glycolytic inactivation

Figure 1 shows flow cytometric analysis using annexin V (horizontal axis) and rhodamine 123 (vertical axis) to examine the effects of glycolysis inhibition on Friend leukemic cells with or without R-PK mutation. SLC3 showed spontaneous apoptosis during routine passage, and apoptosis preceded mitochondrial dysfunction in the R-PK–deficient erythroleukemia cells as reported previously [6]. The result showed that a part of apoptotic cells kept similar mitochondrial transmembrane potentials and that SLC3 were much more susceptible to glucose deprivation as well as 2-DG.

Overexpression of wild-type R-PK decreases apoptosis of SLC3

In order to evaluate how wild-type R-PK rescues apoptotic phenotypes, we established two stable transfectants of SLC3 with overexpression of the human R-PK cDNA. Figure 2 shows RT-PCR and Western blot analysis of a parental SLC3 and SLC3-hRPK.Hi (hRPK.Hi) and SLC3-hRPK.Lo (hRPK.Lo). As shown in Figure 2A, the expression level of the transgene was higher in hRPK.Hi than hRPK.Lo. Overexpression of human R-PK suppressed endogenous R-PK expression as observed in the lane of hRPK.Hi.

Enzymatic analysis of transfectants revealed that PK activities of hRPK.Lo and Hi were 17.2 and 24.2 IU/mg protein, respectively. The PK activity of hRPK.Hi was almost comparable to parental SLC3, 23.5 IU/mg protein. It should be noted that endogenous LDH activity was decreased by transgene expression, leading to a PK/LDH ratio increase from 0.4 (SLC3) to 0.48 (hRPK.Lo) and 0.6 (hRPK.Hi).

We evaluated apoptosis of the two transfectants by cell cycle analysis. Figure 2C shows that the expression of wild-type R-PK decreased the number of cells at the sub-G_0/G_1 stage. While hRPK.Lo showed almost the same number of sub-G_0/G_1 cells (55.5%) as SLC3 (57.4%), only 19.3% of hRPK.Hi were arrested at the sub G_1-stage. Because apoptotic cells were rescued from apoptosis in an R-PK expression level-dependent manner, it is most likely that R-PK activity is required to suppress apoptosis of erythroid cells.

Microarray analysis elucidates the differential expression of genes involved in reactive oxygen species removal, cell cycle, and apoptosis

Gene expression profiles between the two transfectants and the parental SLC3 cell line were analyzed by DNA microarray analysis. After exchanging culture medium, SLC3, hRPK.Lo, and Hi were sampled at 24 and 67 hours, which were the phase of reentry into cell cycling and of subconfluence, respectively. Transgene expression upregulated only about 2% (469 probe sets) of genes, whereas approximately 25% (5754 probe sets) of genes were downregulated both in hRPK.Hi and hRPK.Lo at 24 and/or 67hours. As shown in Figure 3B, major categories of the downregulated genes involved the cell cycle, development, and apoptosis. Proapoptotic genes including *Bad*, *Bnip3*, and *Bnip3l*, as well as *Casp 2, 6, 7,* and *8* were downregulated (Figs. 3A and 4).

Genes of key glycolytic enzymes such as hexokinase-2 (*Hk2*), phosphofructokinase (*Pfkl*), phosphoglycerate kinase (*Pgk1*), and PK (*Pklr*) were downregulated, and expression levels were characteristically decreased after 67 hours of transfection, suggesting that suppression requires protein synthesis.

It should be noted that genes for antioxidant protein, such as peroxiredoxin 1 (*Prdx1*) and related genes, such as catalase (*Cat*), thioredoxin reductase 1 (*Txnrd1*), and glutaredoxin 1 (*Glrx1*), which have a role in the modulation of oxidative stress, are also downregulated. As for *Prdx2*, expression change by the transgene was not evident. Intracellular reactive oxygen species (ROS) are known to cause DNA damage, inducing the expression of DNA repair genes. In this experiment, expressions of genes involved in DNA repair were decreased, including *Brca1*, *Brca2*, and *Rad51*.

PK gene mutation and glycolytic inhibition by 2-DG augment intracellular ROS

We examined intracellular ROS in SLC cells and control CBA2 cells by 2′,7′-dichlorofluorescin-diacetate (DCFH-DA), an indicator of the intracellular formation of hydrogen peroxide and free radicals. Nonfluorescent DCFH-DA turns into DCFH (2′,7′-dichlorofluorescin) in the presence of hydrogen peroxide, and then DCFH is quickly photo-oxidized to fluorescent DCF (2′,7′-dichlorofluorescein).

Figure 5A shows that SLC3 is hypersensitive to a glycolytic inhibitor, 2-DG, producing intracellular DCF by adding 1 mM 2-DG. In contrast, control CBA2 cells do not produce DCF even at 10 mM 2-DG for 30 minutes.

Reduced glutathione (GSH) is an important antioxidant in erythrocytes. GSH is produced by a two-step enzymatic reaction involving γ-glutamylcystein synthetase and glutathione synthetase (GSH-S). Apoptosis induced either by the glycolytic gene mutation (SLC3) or the glycolytic inhibitor (CBA with 2-DG) was suppressed by preincubation with the glutathione precursor, NAC (Fig. 5B). Finally, the

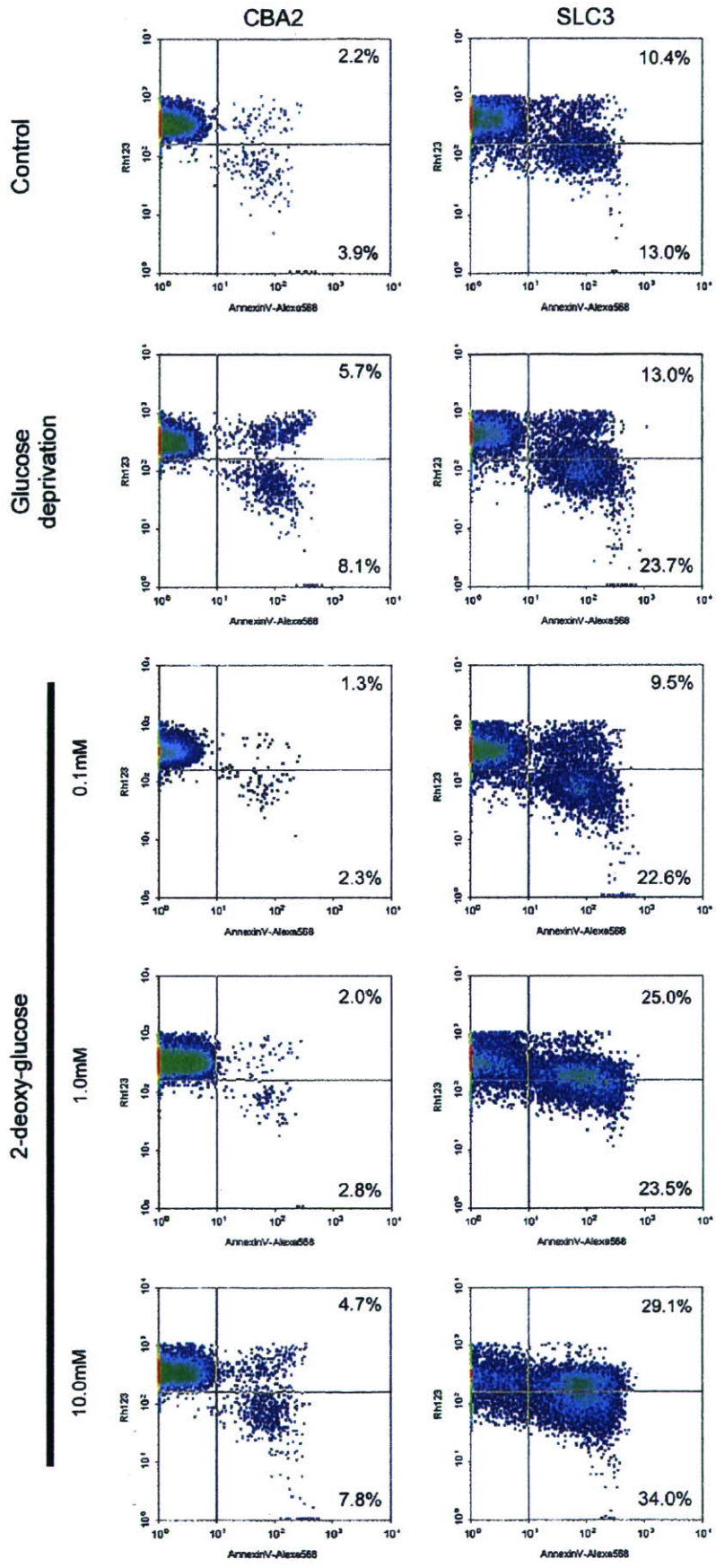
CBA2
SLC3
Control
Glucose deprivation
2-deoxy-glucose
0.1mM
1.0mM
10.0mM
2.2%
3.9%
10.4%
13.0%
5.7%
8.1%
13.0%
23.7%
1.3%
2.3%
9.5%
22.6%
2.0%
2.8%
25.0%
23.5%
4.7%
7.8%
29.1%
34.0%
Rh123
AnnexinV-Alexa568

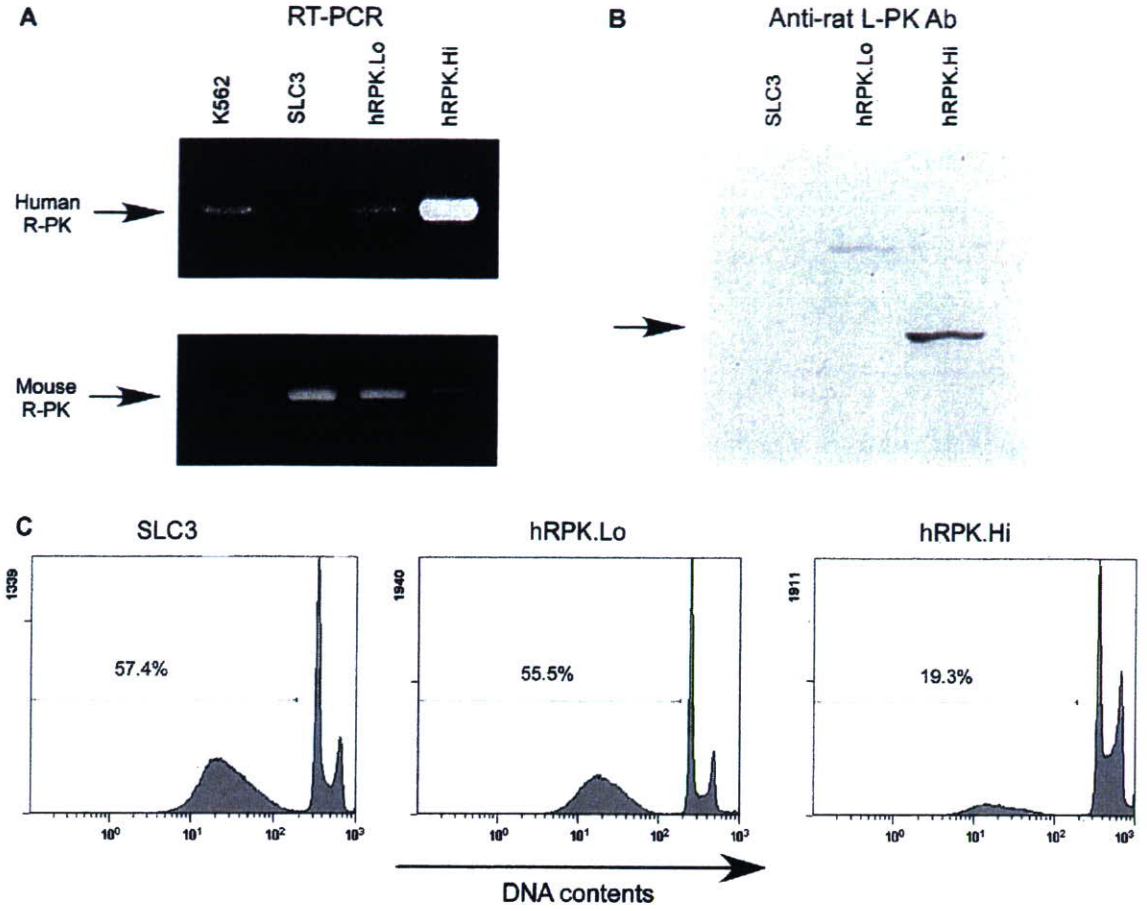

Figure 2. Establishment of the transfectants, SLC3-hRPK.Hi (hRPK.Hi) and SLC3.hRPK.Lo (hRPK.Lo), by introducing the human red blood cell type-pyruvate kinase (R-PK) gene into murine R-PK−deficient cells. Transgene-expression was confirmed by reverse transcriptase polymerase chain reaction (**A**) and Western blotting (**B**). The expression level of hRPK.Hi was higher than that of hRPK.Lo. (**C**) Apoptosis induction in the PK-deficient cells and transfectants. Transfected human R-PK recovered the glycolytic function and showed reduced spontaneous apoptotic changes. The numbers in figures represent the apoptotic change ratio.

forced overexpression of the PK gene reduced intracellular ROS in an expression-level dependent manner (Fig. 5C).

Discussion

Overexpression of human R-PK in SLC3 results in the reduction of apoptotic cells (Fig. 2C), and DNA microarray analysis showed that genes involved in the cell cycle, DNA repair, and antioxidants were downregulated. In general, gene expression levels of transfectants were lower than that of SLC3 (Fig. 3). However, aberrant apoptosis and invalid cell proliferation were restrained in the transfectants. These observations suggested that the cellular activity was not suppressed but was reverted to the normal level by the transgene. It is most likely that the candidate genes suppressed in transfectants were induced in R-PK mutant cells.

Although there were several candidate genes attributing to apoptosis-induction in SLC3, it was still unclear whether these genes were associated with each other or independent. However, there was a possibility that a signal cross-talk phenomenon occurred [14]. *Bad*, a gene encoding a member of the Bcl2-family proapoptotic molecules in mitochondria was significantly downregulated by the transgene (Figs. 3A and 4). Danial et al. [15] reported that *Bad*, BCL2-antagonist of cell death, formed a functional holoenzyme complex together with several molecules, such as glucokinase (hexokinase-4) in liver mitochondria, and contributed to apoptosis induction by glucose deprivation. Our observation suggested that *Bad*

Figure 1. Apoptosis induced by glycolytic inhibition in erythroid cell lines. Glucose deprivation or exposure to 2-deoxyglucose inhibits glycolysis and finally causes apoptosis. The red blood cell type-pyruvate kinase (R-PK)−deficient erythroid cell line (SLC3) is more susceptible than wild-type cells (CBA2) in these conditions. The horizontal axis shows AnnexinV-Arexa568 (= apoptotic change) and the vertical axis shows Rhodamin123 fluorescence (= mitochondrial membrane potential).

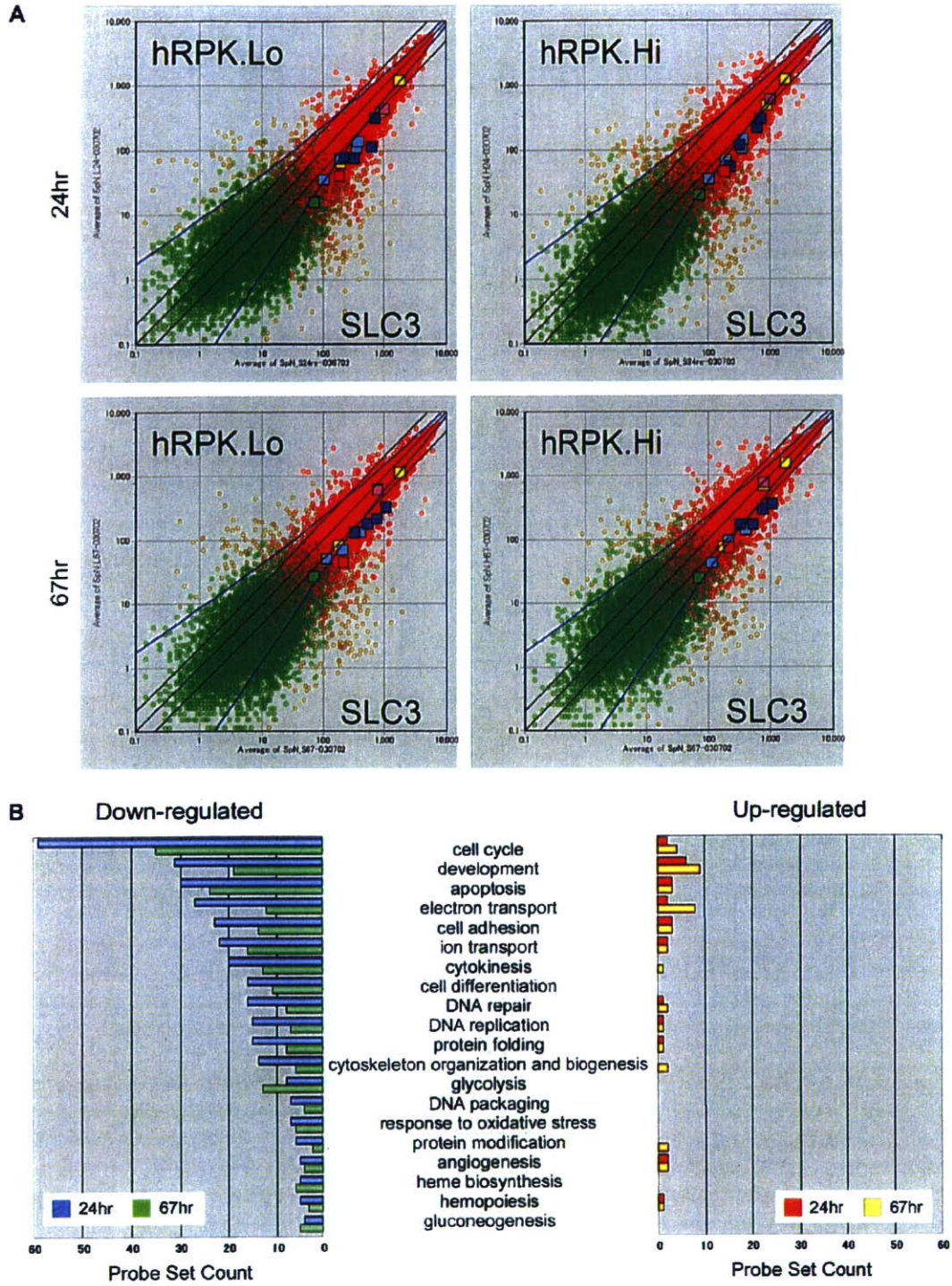

Figure 3. Genome-wide expression analysis of the glycolysis defect. Analysis was performed using the Affymetrix GeneChip Mouse Expression Array 430A, which contains about 20,000 genes. (**A**) Scatter plot between SLC3 and hRPK transfectants at 24 or 67 hours. The open circle shows the expression level of every probe set. The color shows these probabilities provided by the Affymetrix GeneChip Operation System: red means good and green means poor. The colored squares show *Bad* (red), *Bnip3* and *Bnip3l* (blue), *hif1a* (green), *Brca1* and *Brca2* (aqua), *Prdx1* (pink) and *Txnl1* (yellow), respectively. The black lines show twofold, onefold, and 0.5-fold, respectively, and the blue lines show the empirical threshold level. (**B**) The categorized aggregate graph. All probe sets were categorized by the Biological Process Ontology keywords provided by the Gene Ontology project (http://www.geneontology.org/). Up- or downregulation was determined by the spot location in the scatter plotting. Compared with the empirical threshold lines, the upper spots show upregulated genes and the lower spots show downregulated genes.

A Down-regulated Genes

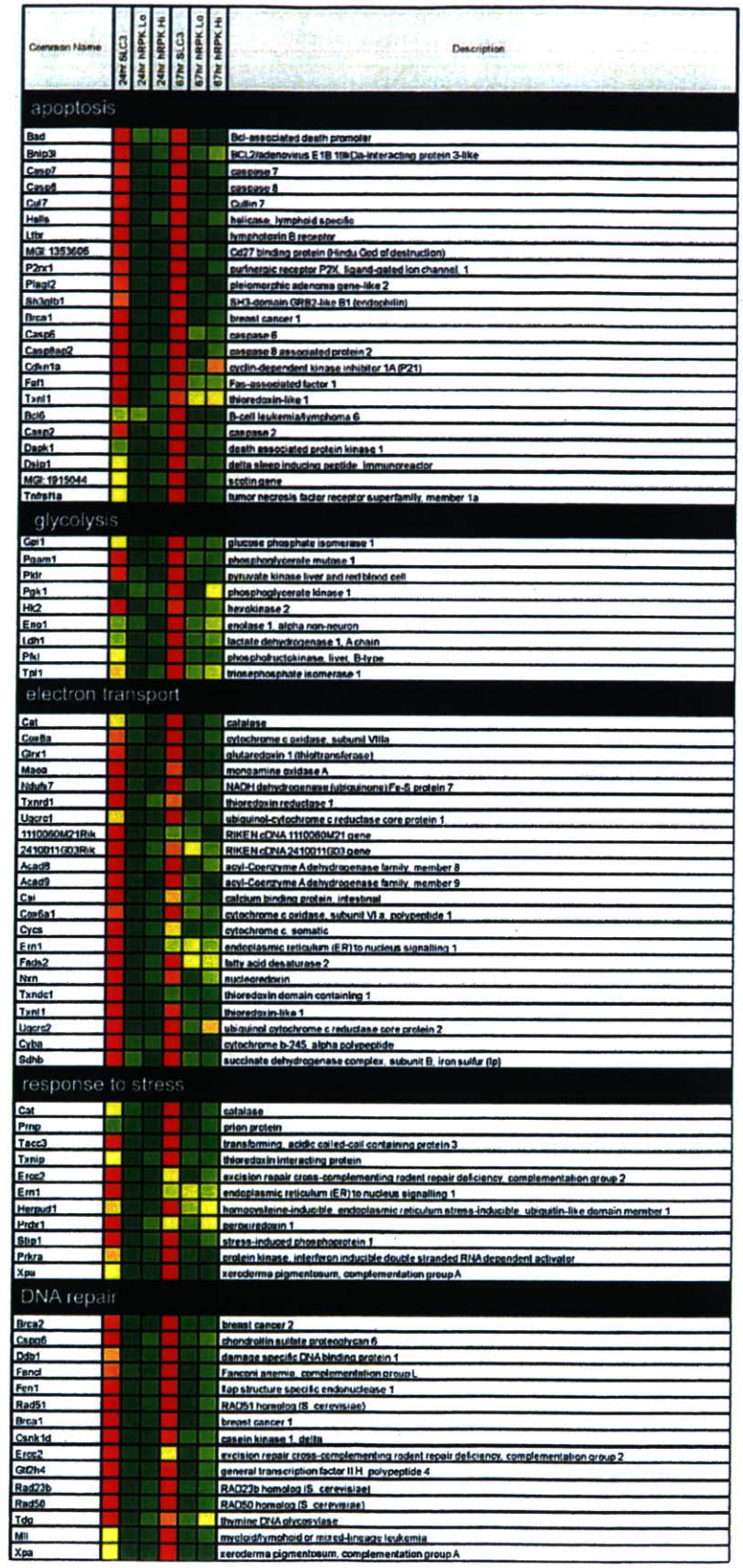

Common Name	24hr SLC3	24hr hRPK.Lo	24hr hRPK.Hi	67hr SLC3	67hr hRPK.Lo	67hr hRPK.Hi	Description
apoptosis							
Bad							Bcl-associated death promoter
Bnip3l							BCL2/adenovirus E1B 19kDa-interacting protein 3-like
Casp7							caspase 7
Casp8							caspase 8
Cul7							Cullin 7
Hells							helicase, lymphoid specific
Ltbr							lymphotoxin B receptor
MGI:1353606							Cd77 binding protein (Hindu God of destruction)
P2rx1							purinergic receptor P2X, ligand-gated ion channel, 1
Plagl2							pleiomorphic adenoma gene-like 2
Sh3glb1							SH3-domain GRB2-like B1 (endophilin)
Brca1							breast cancer 1
Casp6							caspase 6
Caspap2							caspase 8 associated protein 2
Cdkn1a							cyclin-dependent kinase inhibitor 1A (P21)
Faf1							Fas-associated factor 1
Txnl1							thioredoxin-like 1
Bcl6							B-cell leukemia/lymphoma 6
Casp2							caspase 2
Dapk1							death associated protein kinase 1
Dsip1							delta sleep inducing peptide, immunoreactor
MGI:1915044							scotin gene
Tnfrsf1a							tumor necrosis factor receptor superfamily, member 1a
glycolysis							
Gpi1							glucose phosphate isomerase 1
Pgam1							phosphoglycerate mutase 1
Pklr							pyruvate kinase liver and red blood cell
Pgk1							phosphoglycerate kinase 1
Hk2							hexokinase 2
Eno1							enolase 1, alpha non-neuron
Ldh1							lactate dehydrogenase 1, A chain
Pfkl							phosphofructokinase, liver, B-type
Tpi1							triosephosphate isomerase 1
electron transport							
Cat							catalase
Cox8a							cytochrome c oxidase, subunit VIIIa
Glrx1							glutaredoxin 1 (thioltransferase)
Maoa							monoamine oxidase A
Ndufv7							NADH dehydrogenase (ubiquinone) Fe-S protein 7
Txnrd1							thioredoxin reductase 1
Uqcrc1							ubiquinol-cytochrome c reductase core protein 1
1110060M21Rik							RIKEN cDNA 1110060M21 gene
2410011G03Rik							RIKEN cDNA 2410011G03 gene
Acad8							acyl-Coenzyme A dehydrogenase family, member 8
Acad9							acyl-Coenzyme A dehydrogenase family, member 9
Cai							calcium binding protein, intestinal
Cox6a1							cytochrome c oxidase, subunit VI a, polypeptide 1
Cycs							cytochrome c, somatic
Ern1							endoplasmic reticulum (ER) to nucleus signalling 1
Fads2							fatty acid desaturase 2
Nxn							nucleoredoxin
Txndc1							thioredoxin domain containing 1
Txnl1							thioredoxin-like 1
Uqcrc2							ubiquinol cytochrome c reductase core protein 2
Cyba							cytochrome b-245, alpha polypeptide
Sdhb							succinate dehydrogenase complex, subunit B, iron sulfur (Ip)
response to stress							
Cat							catalase
Prnp							prion protein
Tacc3							transforming, acidic coiled-coil containing protein 3
Txnip							thioredoxin interacting protein
Ercc2							excision repair cross-complementing rodent repair deficiency, complementation group 2
Ern1							endoplasmic reticulum (ER) to nucleus signalling 1
Herpud1							homocysteine-inducible, endoplasmic reticulum stress-inducible, ubiquitin-like domain member 1
Prdx1							peroxiredoxin 1
Stip1							stress-induced phosphoprotein 1
Prkra							protein kinase, interferon inducible double stranded RNA dependent activator
Xpa							xeroderma pigmentosum, complementation group A
DNA repair							
Brca2							breast cancer 2
Cspg6							chondroitin sulfate proteoglycan 6
Ddb1							damage specific DNA binding protein 1
Fancl							Fanconi anemia, complementation group L
Fen1							flap structure specific endonuclease 1
Rad51							RAD51 homolog (S. cerevisiae)
Brca1							breast cancer 1
Csnk1d							casein kinase 1, delta
Ercc2							excision repair cross-complementing rodent repair deficiency, complementation group 2
Gtf2h4							general transcription factor II H, polypeptide 4
Rad23b							RAD23b homolog (S. cerevisiae)
Rad50							RAD50 homolog (S. cerevisiae)
Tdg							thymine DNA glycosylase
Mll							myeloid/lymphoid or mixed-lineage leukemia
Xpa							xeroderma pigmentosum, complementation group A

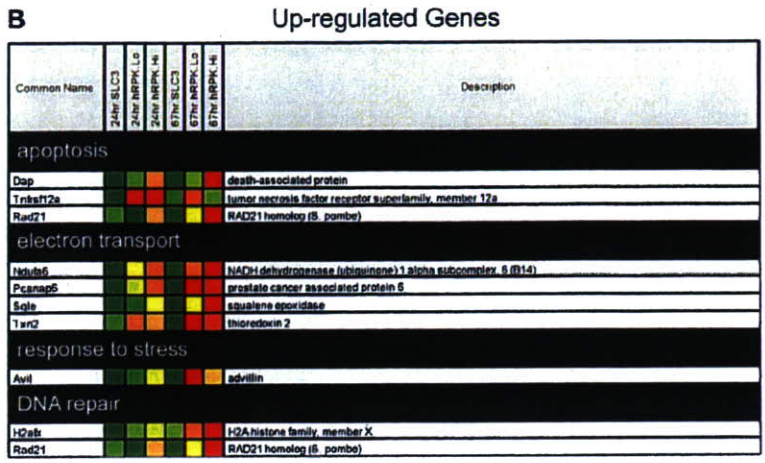

Figure 4. *Continued*

could be involved in the apoptosis induced by glycolysis defect in erythroid cells as well as in the liver.

The genes of apoptosis-inducers related to hypoxia such as *Bnip3* and *Bnip3l*, which are known as inducible genes by hypoxia-inducible factor-1α, were inactivated markedly by the forced expression of the wild-type R-PK gene. Although the extent of downregulation was smaller than for *Bnip3*, *Bnip3l* showed a significant decrease of expression by the transgene (Fig. 3A). Moreover, the downregulation was more obvious at 24 hours, suggesting that these genes may contribute to the initial response caused by a glycolytic defect. These observations strongly suggested that the apoptosis induction by the glycolysis disorder was executed by the *Bnip3-Bnip3l* signal.

It is noticeable that several genes important for responding to oxidative stress are upregulated, suggesting that R-PK deficiency might account for intracellular ROS production. This speculation is supported by the following experimental observations: Firstly, SLC3 cells were more sensitive to glycolytic inhibitions such as glucose deprivation and supplementation with 2-DG (Fig. 1), and these conditions induced ROS production detected by DCFH-DA (Fig. 5A). Apoptotic changes induced by 2-DG were partly rescued by preincubation with the glutathione precursor (Fig. 5B). Finally, transgene expression reduced intracellular ROS in an expression-level–dependent manner (Fig. 5C).

Glycolytic disorders may cause cellular conditions similar to those of hypoxia. Shim et al. [16] reported that induction of the LDH-A gene by c-Myc was advantageous to transformed cells that exist under hypoxic conditions [15]. However, glucose deprivation induces the extensive apoptosis of cells overexpressing c-Myc. Overexpression of LDH-A alone in fibroblasts is sufficient to sensitize cells to this glucose deprivation-induced apoptosis. They proposed a hypothesis that LDH-A was a downstream target of c-Myc that mediates this unique apoptotic phenotype. We noticed that pyruvate was the final product as well as the substrate of the PK and LDH reaction, respectively. Both LDH hyperactivity and PK deficiency may cause the depletion of intracellular pyruvate, suggesting that pyruvate has an important role in preventing apoptosis.

Several studies have revealed that pyruvate acts as an antioxidant and that PK has a protective role against oxidative stress in this respect. Brand et al. [17] reported that proliferating thymocytes mainly depend on energy derived from aerobic glycolysis, and that their sensitivity to 12-myristate 13-acetate–induced ROS production is much lower than that of resting thymocytes, which produce ATP mainly through oxidative phosphorylation. They suggested that pyruvate functions as an ROS scavenger, because the incubation of proliferating thymocytes with pyruvate reduced ROS formation.

The PK-overexpressing neuronal cells could attenuate oxidative stress and maintain cell viability [18]. Lee et al. [19] showed that hydrogen peroxide depleted intracellular GSH in human umbilical vein endothelial cells, and that was prevented by pyruvate but not by L-lactate or aminooxyacetate. The activation of caspases was strongly inhibited by pyruvate, but markedly enhanced by L-lactate and aminooxyacetate, implicating the redox-related antiapoptotic mechanisms of pyruvate. Myocardial ischemia-reperfusion

Figure 4. Representative list of the genes affected by the functional recovery of glycolysis. Genome-wide expression analysis was performed using Affymetrix GeneChip Mouse Expression Array 430A, which contains about 20,000 genes. In the comparison among hRPK.Hi, hRPK.Lo, and SLC3, about 6000 genes were downregulated and about 500 genes were upregulated by the functional recovery of glycolysis at 24 and/or 67 hours after regular passage. These lists contain the affected genes related to apoptosis and/or the oxidative stress response.

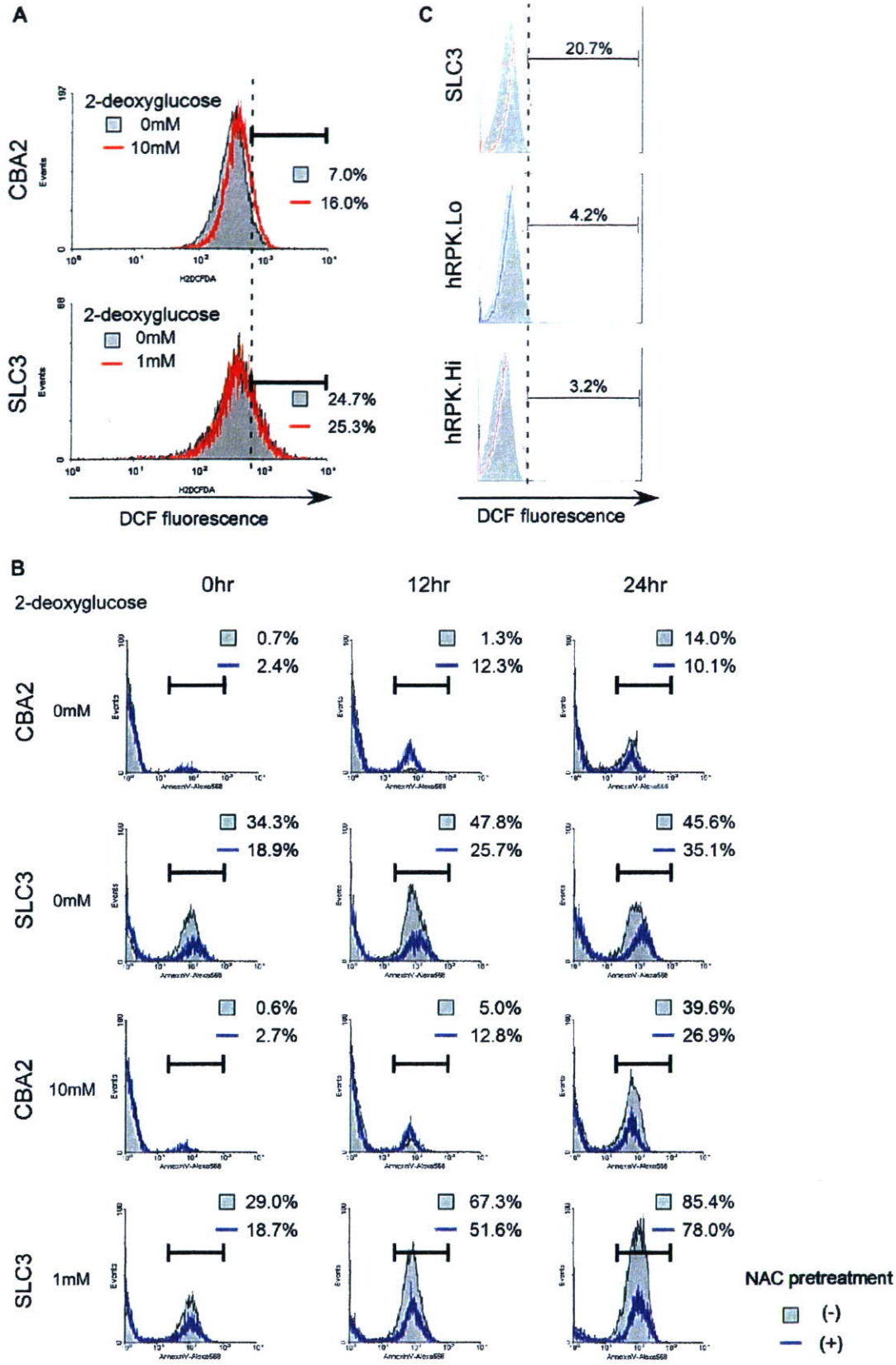
A
CBA2
2-deoxyglucose
0mM
10mM
7.0%
16.0%
SLC3
2-deoxyglucose
0mM
1mM
24.7%
25.3%
H2DCFDA
DCF fluorescence
C
SLC3
20.7%
hRPK.Lo
4.2%
hRPK.Hi
3.2%
DCF fluorescence
B
2-deoxyglucose
0hr
12hr
24hr
CBA2
0mM
0.7%
2.4%
1.3%
12.3%
14.0%
10.1%
SLC3
0mM
34.3%
18.9%
47.8%
25.7%
45.6%
35.1%
CBA2
10mM
0.6%
2.7%
5.0%
12.8%
39.6%
26.9%
SLC3
1mM
29.0%
18.7%
67.3%
51.6%
85.4%
78.0%
NAC pretreatment
(-)
(+)

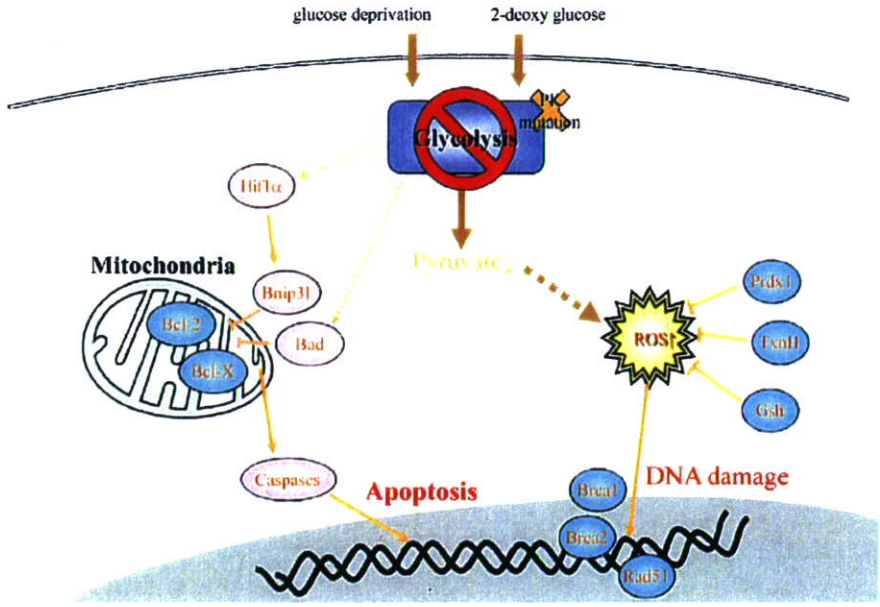

Figure 6. Glycolytic defect causes oxidative stress and hypoxia-like signal activation. Pyruvate, which is final metabolic product of the glycolytic pathway, acts as an antioxidant. Therefore, glycolytic defect elevates intracellular reactive oxygen species (ROS) and causes cellular damage, such as DNA damage and lipid oxidation. At the same time, glycolytic defect is most likely to activate signal transduction through hypoxia-inducible factor-1α (HIF-1α). These cellular responses could be accountable for the apoptosis induced by glycolytic defect.

is reported to be associated with bursts of ROS, such as superoxide radicals, and cardiac superoxide formation can be inhibited by pyruvate [20]. Thus cytotoxicities due to cardiac ischemia-reperfusion ROS can be alleviated by redox reactants such as pyruvate. These results support our present data, which showed that a mutation of the PK gene as well as inhibition of glycolysis by 2-DG augmented intracellular ROS of erythroid cells, leading to apoptosis. Introduction of the wild-type PK gene into SLC3 cells partly reduced ROS and apoptosis (Figs. 2C and 6C).

In human RBC, the most important antioxidant is GSH. Mutations of enzymes involving the synthesis and reduction of GSH, such as γ-glutamylcystein synthetase, GSH-S, glutathione reductase, and glucose-6-phosphate dehydrogenase account for the shortened RBC survival [1,21]. Recently, Neumann et al. [22] and Lee et al. [23] reported the essential roles of both peroxiredoxin (Prdx) 1 and 2 in RBC protection from oxidative stress. The hemolytic anemia of mice with targeted inactivation of *Prdx1* is characterized by an increase in erythrocyte reactive oxygen species, leading to protein oxidation and Heinz body formation. Similarly, the *Prdx2* knockout mice had Heinz body-positive hemolytic anemia with splenomegaly. The dense RBC fractions contained markedly higher levels of ROS. These studies highlighted a pivotal role of *Prdx* as a scavenger of hydrogen peroxide in RBC. *Prdx1* may be concerned with the initial response to glycolytic deficiency, because the gene expression in SLC3 was higher than that in transfectants only at 24 hours (Fig. 3A). The mechanisms responsible for upregulation of *Prdx1* and similar antioxidant enzymes in SLC3 remain to be elucidated.

It is most likely that the main pathogenesis of PK deficiency is decreased ATP production due to impaired glycolysis, resulting in the premature destruction of RBC in the reticuloendothelial system, i.e., extravascular hemolysis. In most cases, hemolysis is partly compensated by enhanced erythropoiesis. We have previously shown that the numbers of hematopoietic progenitors including colony-forming unit (CFU)-erythroid, CFU-granulocyte macrophage, burst-forming unit-erythroid, and CFU-granulocyte-erythrocyte monocyte-megakaryocyte were increased in *Pk-1*^{slc} mice [10]. The proliferation of erythroid progenitors might require

Figure 5. The oxidative stress pathway might play some role in the apoptosis induced by glycolytic disorder. (**A**) The SLC3 cells produce 2′,7′-dichlorofluorescein (DCF) continuously with and without 2-deoxyglucose (2-DG) due to the red blood cell type-pyruvate kinase (R-PK) defect. The control CBA2 cells produce DCF with 10 mM 2-DG for 30 minutes. The gray area shows the nontreated group and the red line shows the treated group with 2-DG. The horizontal axis shows the fluorescence intensity of the DCF. (**B**) The apoptosis induced by glycolytic defect or by glycolysis inhibitor was suppressed by the preincubation with the glutathione precursor, N-acetyl-cysteine (NAC). The gray area shows the nonpretreated group and the blue line shows the pretreated group with NAC. The horizontal axis shows the fluorescence intensity of the Annexin V-Alexa568.

activation of glycolysis in order to suppress intracellular ROS. Therefore, R-PK deficiency becomes a serious problem for erythroid cells to avoid apoptosis. In summary, we concluded that the premature destruction of RBC as well as apoptosis of erythroid progenitors accounts for the pathogenesis of R-PK deficiency.

Although most severe cases die either in utero or during the neonatal period [24,25], there is no curative therapy of PK deficiency except hematopoietic stem cell transplantation [26] at present. Because hematopoietic stem cell transplantation may accompany life-threatening complications, a safer treatment should be considered. Studies on the apoptotic induction of erythroid progenitors in R-PK deficiency may be useful for the identification of molecular targets of causal treatment.

Acknowledgments

We are indebted to Takako Hamada and Miyuki Yuda for their excellent technical assistance. This work was supported in part by a Grant-in-Aid for Scientific Research from the Japan Society of the Promotion of Science (project nos. 14570131 and 16590254), and also by a Scientific Research Grant from the Ministry of Health, Labor and Welfare (H15-kagaku-002, H18-kagaku-ippan-001), Japan.

References

1. Hirono A, Kanno H, Miwa S, Beutler E. Pyruvate kinase deficiency and other enzymopathies of the erythrocyte. In: Scriver CR, Beaudet AL, Sly WS, Valle D, eds. The Metabolic & Molecular Bases of Inherited Disease. 8th ed. New York: McGraw-Hill; 2001. p. 4637–4664.
2. Takegawa S, Fujii H, Miwa S. Change of pyruvate kinase isozymes from M2- to L-type during development of the RBC. Br J Haematol. 1983;54:467–474.
3. Max-Audit I, Kechemir D, Mitjavila MT, Vainchenker W, Rotten D, Rosa R. Pyruvate kinase synthesis and degradation by normal and pathologic cells during erythroid maturation. Blood. 1988;72: 1039–1044.
4. Tanaka KR, Zerez CR. RBC enzymopathies of the glycolytic pathway. Semin Hematol. 1990;27:165–185.
5. Zanella A, Fermo E, Bianchi P, Valentini G. RBC pyruvate kinase deficiency: molecular and clinical aspects. Br J Haematol. 2005;130: 11–25.
6. Aisaki K, Kanno H, Oyaizu N, Hara Y, Miwa S, Ikawa Y. Apoptotic changes precede mitochondrial dysfunction in red cell-type pyruvate kinase mutant mouse erythroleukemia cell lines. Jpn J Cancer Res. 1999;90:171–179.
7. Morimoto M, Kanno H, Asai H, et al. Pyruvate kinase deficiency of mice associated with nonspherocytic hemolytic anemia and cure of the anemia by marrow transplantation without host irradiation. Blood. 1995;86:4323–4330.
8. Kanno H, Morimoto M, Fujii H, et al. Primary structure of murine red blood cell-type pyruvate kinase (PK) and molecular characterization of PK deficiency identified in the CBA strain. Blood. 1995;86: 3205–3210.
9. Aizawa S, Kohdera U, Hiramoto M, et al. Ineffective erythropoiesis in the spleen of a patient with pyruvate kinase deficiency. Am J Hematol. 2003;74:68–72.
10. Aizawa S, Harada T, Kanbe E, et al. Ineffective erythropoiesis in mutant mice with deficient pyruvate kinase activity. Exp Hematol. 2005; 33:1292–1298.
11. Kanno H, Fujii H, Hirono A, Miwa S. cDNA cloning of human R-type pyruvate kinase and identification of a single amino acid substitution (Thr384→Met) affecting enzymatic stability in a pyruvate kinase variant (PK Tokyo) associated with hereditary hemolytic anemia. Proc Natl Acad Sci U S A. 1991;88:8218–8221.
12. Beutler E, Blume KG, Kaplan JC, Loehr GW, Ramot B, Valentine WN. International Committee for Standardization in Haematology: recommended methods for red cell enzyme analysis. Br J Haematol. 1977;35:331–340.
13. Kanno J, Aisaki K, Igarashi K, et al. "Per cell" normalization method for mRNA measurement by quantitative PCR and microarrays. BMC Genomics. 2006;29:64.
14. Krones A, Jungermann K, Kietzmann T. Cross-talk between the signals hypoxia and glucose at the glucose response element of the L-type pyruvate kinase gene. Endocrinology. 2001;142:2707–2718.
15. Danial NN, Gramm CF, Scorrano L, et al. BAD and glucokinase reside in a mitochondrial complex that integrates glycolysis and apoptosis. Nature. 2003;424:952–956.
16. Shim H, Chun YS, Lewis BC, Dang CV. A unique glucose-dependent apoptotic pathway induced by c-Myc. Proc Natl Acad Sci U S A. 1998;95:1511–1516.
17. Brand K, Netzker R, Aulwurm U, et al. Control of thymocyte proliferation via redox-regulated expression of glycolytic genes. Redox Rep. 2000;5:52–54.
18. Shimizu T, Uehara T, Nomura Y. Possible involvement of pyruvate kinase in acquisition of tolerance to hypoxic stress in glial cells. J Neurochem. 2004;91:167–175.
19. Lee YJ, Kang IJ, Bunger R, Kang YH. Mechanisms of pyruvate inhibition of oxidant-induced apoptosis in human endothelial cells. Microvasc Res. 2003;66:91–101.
20. Basing E, Summer O, Schemer M, Bunger R. Antioxidant pyruvate inhibits cardiac formation of reactive oxygen species through changes in redox state. Am J Physiol Heart Circ Physiol. 2000;279:H2431–H2438.
21. Luzzatto L, Mehta A, Vulliamy T. Glucose 6-phosphate dehydrogenase. In: Scriver CR, Beaudet AL, Sly WS, Valle D, eds. The Metabolic & Molecular Bases of Inherited Disease. 8th ed.. New York: McGraw-Hill; 2001. p. 4517–4554.
22. Neumann CA, Krause DS, Carman CV, et al. Essential role for the peroxiredoxin Prdx1 in erythrocyte antioxidant defense and tumour suppression. Nature. 2003;424:561–565.
23. Lee TH, Kim SU, Yu SL, et al. Peroxiredoxin II is essential for sustaining life span of erythrocytes in mice. Blood. 2003;101:5033–5038.
24. Ferreira P, Morais L, Costa R, et al. Hydrops fetalis associated with erythrocyte pyruvate kinase deficiency. Eur J Pediatr. 2000;159: 481–482.
25. Bowman HS, McKusick VA, Dronamraju KR. Pyruvate kinase deficient hemolytic anemia in an Amish isolate. Am J Hum Genet. 1965;17:1–8.
26. Tanphaichitr VS, Suvatte V, Issaragrisil S, et al. Successful bone marrow transplantation in a child with red blood cell pyruvate kinase deficiency. Bone Marrow Transplant. 2000;26:689–690.

0026-895X/07/7205-1171–1180$20.00
MOLECULAR PHARMACOLOGY
Copyright © 2007 The American Society for Pharmacology and Experimental Therapeutics
Mol Pharmacol 72:1171–1180, 2007

Vol. 72, No. 5
38836/3268509
Printed in U.S.A.

Evaluation of Action Mechanisms of Toxic Chemicals Using JFCR39, a Panel of Human Cancer Cell Lines[S]

Noriyuki Nakatsu, Tomoki Nakamura, Kanami Yamazaki, Soutaro Sadahiro, Hiroyasu Makuuchi, Jun Kanno, and Takao Yamori

Division of Molecular Pharmacology, Cancer Chemotherapy Center, Japanese Foundation for Cancer Research, Koto-ku, Tokyo, Japan (N.N., T.N., K.Y., T.Y.); Division of Cellular and Molecular Toxicology, Biological Safety Research Center, National Institute of Health Sciences, Setagaya-ku, Tokyo, Japan (N.N., J.K.); and Second Department of Surgery, Tokai University School of Medicine, Boseidai, Isehara-City, Kanagawa, Japan (T.N., S.S., H.M.)

Received June 6, 2007; accepted August 16, 2007

ABSTRACT

We previously established a panel of human cancer cell lines, JFCR39, coupled to an anticancer drug activity database; this panel is comparable with the NCI60 panel developed by the National Cancer Institute. The JFCR39 system can be used to predict the molecular targets or evaluate the action mechanisms of the test compounds by comparing their cell growth inhibition profiles (i.e., fingerprints) with those of the standard anticancer drugs using the COMPARE program. In this study, we used this drug activity database-coupled JFCR39 system to evaluate the action mechanisms of various chemical compounds, including toxic chemicals, agricultural chemicals, drugs, and synthetic intermediates. Fingerprints of 130 chemicals were determined and stored in the database. Sixty-nine of 130 chemicals (~60%) satisfied our criteria for the further analysis and were classified by cluster analysis of the fingerprints of these chemicals and several standard anticancer drugs into the following three clusters: 1) anticancer drugs, 2) chemicals that shared similar action mechanisms (for example, ouabain and digoxin), and 3) chemicals whose action mechanisms were unknown. These results suggested that chemicals belonging to a cluster (i.e., a cluster of toxic chemicals, a cluster of anticancer drugs, etc.) shared similar action mechanism. In summary, the JFCR39 system can classify chemicals based on their fingerprints, even when their action mechanisms are unknown, and it is highly probable that the chemicals within a cluster share common action mechanisms.

Determining the action mechanism or identifying the molecular target of a chemical with pharmacological activity or adverse side effects is highly desirable. Although various test methods are currently available for determining the action mechanisms of chemicals, such as methods based on animal models, methods based on cellular models, bacterial mutagenicity test, the uterotropic assay (Kanno et al., 2002), Hershberger test (Hershberger et al., 1953), and the reporter assay for the nuclear receptor agonists, determination of the action mechanisms of pharmacologically active chemicals, including the toxic chemicals, is still a difficult and challenging task. Therefore, it is highly desirable to develop efficient test methods for evaluating toxicity of chemicals.

A number of screening methods are currently available for discovering new anticancer drugs. One very powerful and unique approach using multiple cancer cell lines was developed at NCI (Paull et al., 1989; Weinstein et al., 1992, 1997) and in our laboratory (Yamori et al., 1999; Dan et al., 2002, 2003; Yamori, 2003; Nakatsu et al., 2005; Akashi and Yamori, 2007; Akashi et al., 2007; Nakamura et al., 2007). This bioinformatics-based approach enables mechanism-oriented evaluation of anticancer drugs. For example, we can evaluate the cell toxicity in vitro by determining the 50% growth inhibition (GI50), total growth inhibition, and 50% lethal concentration across a panel of 39 human cancer cell lines (JFCR39). We can also predict the molecular targets or evaluate the action mechanisms of the test compounds by comparing the cell growth inhibition profiles (termed "fingerprints") across the panel for these compounds with those of

This work was supported in part by Grant-in-Aid 17390032 for Scientific Research (B) from Japan Society for the Promotion of Science (to T.Y.); Ministry of Health, Labor, and Welfare Grants-in-Aid H15-kagaku-002, H16-kagaku-003 (to T.Y. and J.K.); Grant-in-Aid 18015049 of the Priority Area "Cancer" from the Ministry of Education, Culture, Sports, Science and Technology of Japan (to T.Y.); and grant 05-13 from National Institute of Biomedical Innovation Japan (to T.Y.)

N. N. and T. N. equally contributed to this study.

Article, publication date, and citation information can be found at http://molpharm.aspetjournals.org.
doi:10.1124/mol.107.038836.

[S] The online version of this article (available at http://molpharm.aspetjournals.org) contains supplemental material.

ABBREVIATIONS: GI50, 50% growth inhibition concentration; GI50, 50% growth inhibition; SN-38, 7-ethyl-10-hydroxycamptothecin; SV-NN, snake venom from *N. nigricollis*; SV-NNK; snake venom from *N. naja kaouthia*.

TABLE 1
List of chemicals tested. Chemical names, abbreviations, and applications/targets/mechanisms of the test compounds are summarized.

JCI No	Name	Abbreviation	Application/Target/Mechanism
−691	Trioctyltin	TOT	Organotin
−690	Triphenyltin	TPT	Organotin
−689	Dibutyltin		Organotin
−688	AM-580		RARα
−687	TTNPB		RAR
−686	13-*cis* Retinoic acid	13-*cis*	RAR
−607	Methoprene		Agricultural chemical
−606	Methoprene acid		RXR
−605	5-aza-2′-deoxycytidine	5-AzaC	Methylation
−604	Carbaryl		Agricultural chemical
−603	Acephate		Agricultural chemical
−602	Sodium arsenite		Agricultural chemical
−601	Testosterone propionate	TP	Testosterone
−600	Ethynyl estradiol	EE	Estrogenic
−599	Thiram		Agricultural chemical
−598	Dimethylformamide	DMF	Solvent
−568	α-Bungarotoxin	αBuTX	Neurotoxin
−567	Snake venom from *Trimeresurus flavoviridis*	SV-TF	Snake venom
−566	Snake venom from *Crotalus atrox*	SV-CA	Snake venom
−565	Snake venom from *Agkistrodon halys blomhoffii*	SV-AHB	Snake venom
−564	Dexamethasone	DEX	Steroid
−563	3-Methylcholanthrene	3-MC	Teratogenicity/carcinogenicity
−562	*N*-Ethyl-*N*-nitrosourea	ENU	Teratogenicity/carcinogenicity
−561	Diethylnitrosamine	DEN	Teratogenicity/carcinogenicity
−560	All *trans*-retinoic acid	ATRA	RAR + RXR
−559	9-cis Retinoic acid	9-cis	RAR
−558	Levothyroxine	T4	Thyroid hormone
−557	3-Amino-1*H*-1,2,4-triazole	3AST	Agricultural chemical
−555	2-Vinylpyridine	2VP	Synthetic intermediate
−553	Phenobarbital	PB	Antiepileptic
−552	Acetaminophen	APAP	Analgetic
−551	Isoniazid		Phthisic
−549	4-Ethylnitrobenzene	4ENB	Synthetic intermediate
−548	1,2-Dichloro-3-nitrobenzene	1,2DC3NB	Pigment/synthetic intermediate
−546	*N*-Methylaniline	NMA	Synthetic intermediate
−545	2-Aminomethylpyridine	2AMP	Synthetic intermediate
−544	1*H*-1,2,4-Triazole		Synthetic intermediate
−543	1*H*-1,2,3-Triazole		Synthetic intermediate
−542	4-Amino-2,6-dichlorophenol	4A2,6DCP	Synthetic intermediate
−541	2,4-Dinitrophenol	2,4 DNP	Agricultural chemical
−513	Capsaicin		Food constituent
−485	2-Methoxyestradiol		Estrogenic
−466	Colcemid		Spindle inhibitor
−465	2,4-Dinitrochlorobenzene	2,4DCB	Pigment/mutagenesis
−464	Troglitazone		Diabetic
−463	Clofibrate		Antilipemic
−459	Bis(2-ethylhexyl)phthalate	DEHP	Plasticizer
−458	Thiourea		Agricultural chemical
−447	Cacodylic acid		Agricultural chemical
−446	Amitrole		Agricultural chemical
−445	4-Octylphenol	OP	Reproductive effector
−444	2,6-Dimethylaniline	2,6-Xylidene	Natural product
−443	1,2-Dibromo-3-chloropropane	DBCP	Agricultural chemical
−442	1,1-Dimethylhydrazine	1,1DMH	Reproductive effector
−441	Sulfanylamide		Agricultural chemical
−440	Streptozotocin		Agricultural chemical
−439	Spironolactone		Aldosterone antagonist
−438	*para*-Aminoazobenzene	pAAB	Pigment/mutagenicity/carcinogenicity
−437	*para*-Cresidine		Pigment/carcinogenicity
−436	Neostigmine bromide		Parasympathomimetics
−435	*para*-Dichlorobenzene	pDCB	Pigment/Agricultural chemical
−434	Phenytoin		Antiepileptic
−433	*ortho*-Toluidine	oToluidine	Pigment
−432	Imipramine		Antidepressant
−431	Cobalt chloride		Teratogenicity/mutagenicity
−428	Atrazine		Agricultural chemical
−427	Propylthiouracil		Teratogenicity/carcinogenicity
−426	Thalidomide (L + D)		Teratogenicity
−425	Carbon tetrachloride	CCl_4	Teratogenicity/carcinogenicity
−424	Hydroquinone		Oxidative stress
−423	Monocrotaline		Mutagenicity/carcinogenicity
−422	Vinyl chloride		Carcinogenicity
−421	Tributyltin chloride	TBT	Ship bottom paint/organotin
−420	Valproic acid		Antiepileptic
−419	Benzene		Carcinogenicity